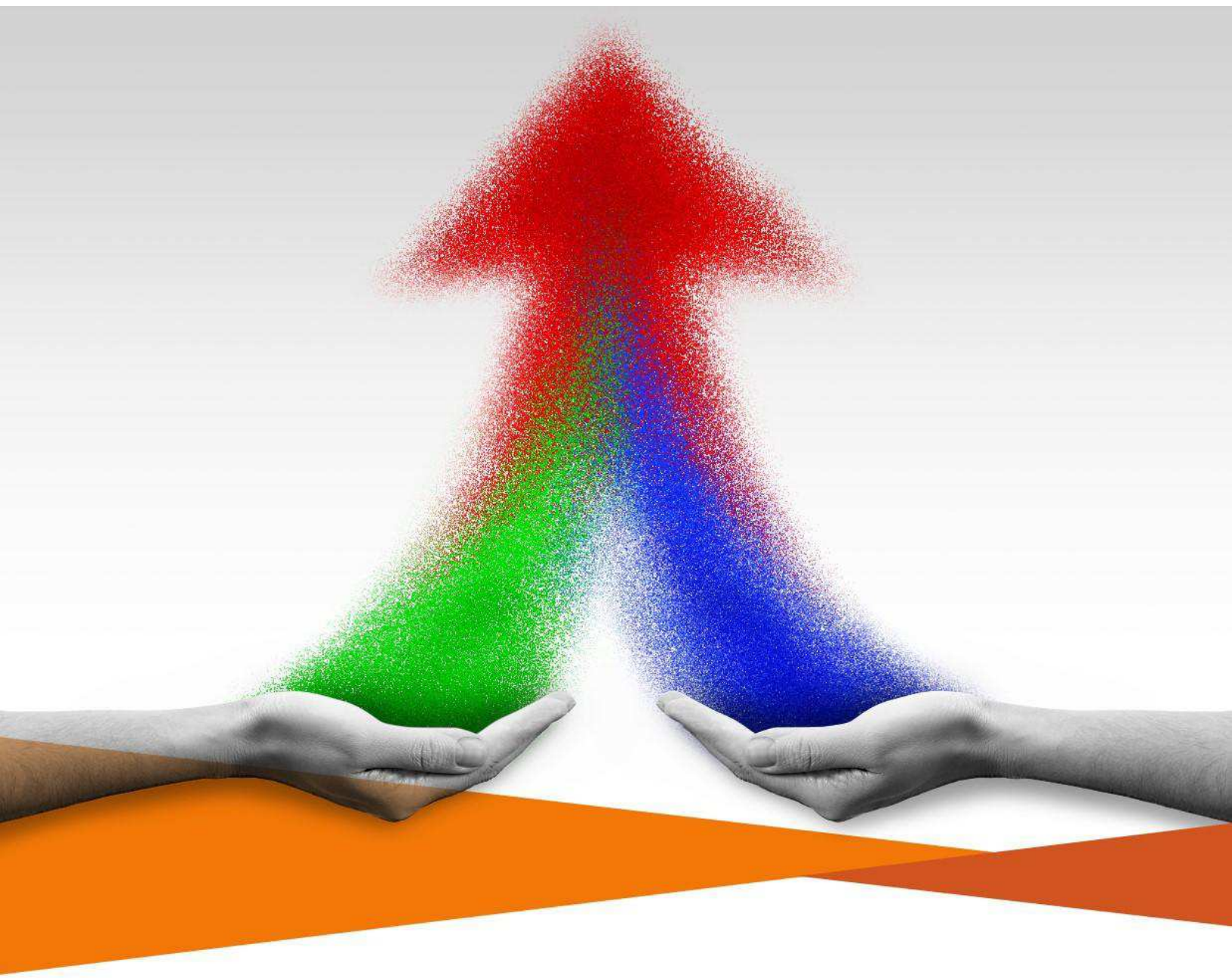

Supporting your research with our capabilities

BD Accuri™ C6 Plus Personal Flow Cytometer

BD FACSCelesta™ Cell Analyzer

BD LSRFortessa™ X-20 Cell Analyzer

BD FACSMelody™ Cell Sorter

One of the largest portfolios of reagents

Learn more>

BD

IJC
International Journal of Cancer

Establishment and characterization of MRT cell lines from genetically engineered mouse models and the influence of genetic background on their development

Yasumichi Kuwahara[1], E. Lorena Mora-Blanco[2], Fatima Banine[3], Arlin B. Rogers[1,4], Christopher Fletcher[5], Larry S. Sherman[3], Charles W. M. Roberts[2] and Bernard E. Weissman[1,4]

[1] UNC-Lineberger Comprehensive Cancer Center, University of North Carolina, Chapel Hill, NC
[2] Department of Pediatric Oncology, Dana-Farber Cancer Institute, Children's Hospital Boston and Harvard University, Boston, MA
[3] Division of Neuroscience, Oregon National Primate Research Center, Oregon Health and Science University, Beaverton, OR
[4] Department of Pathology and Laboratory Medicine, University of North Carolina, Chapel Hill, NC
[5] Department of Pathology, Brigham and Women's Hospital, Boston, MA

Malignant rhabdoid tumors (MRTs) are rare, aggressive cancers occuring in young children primarily through inactivation of the *SNF5(INI1, SMARCB1)* tumor suppressor gene. We and others have demonstrated that mice heterozygous for a *Snf5* null allele develop MRTs with partial penetrance. We have also shown that $Snf5^{+/-}$ mice that lack expression of the pRb family, due to TgT_{121} transgene expression, develop MRTs with increased penetrance and decreased latency. Here, we report that altering the genetic background has substantial effects upon MRT development in $Snf5^{+/-}$ and TgT_{121};$Snf5^{+/-}$ mice, with a mixed F1 background resulting in increased latency and the appearance of brain tumors. We also report the establishment of the first mouse MRT cell lines that recapitulate many features of their human counterparts. Our studies provide further insight into the genetic influences on MRT development as well as provide valuable new cell culture and genetically engineered mouse models for the study of CNS-MRT etiology.

Cancer Cell Biology

Malignant rhabdoid tumors (MRTs) are highly aggressive pediatric malignancies that can arise in the kidneys and soft tissues throughout the body, as well as in the central nervous system, where they are referred to as atypical teratoid/rhabdoid tumors or AT/RTs.[1] Patients may develop more than one primary tumor as ~10–15% of patients with renal MRTs also develop independent primary tumors of the CNS.[2] These cancers are extremely aggressive, with most patients perishing within 1 year of diagnosis.[3] Therefore, new treatment approaches for this disease remain a high priority.

Rhabdoid cells have distinctive cellular characteristics including large vesicular nuclei, a prominent single nucleolus, and globular eosinophilic cytoplasmic inclusions. Because MRTs typically consist of poorly differentiated cells with a few admixed rhabdoid cells, diagnosis based on histology alone has proven difficult. However, recent studies have shown that virtually all MRTs lose expression of the *SNF5/INI1/BAF47/SMARCB1* gene providing a useful diagnostic marker.[4,5] The *SNF5* gene, which encodes the smallest member of the SWI/SNF chromatin remodeling complex, localizes to 22q11.2. The SNF5 protein interacts with many transcription regulators and viral proteins, such as c-MYC, p53 and HIV-IN.[6] The SNF5 protein is highly conserved among different species with complete identity between mouse and human proteins.[7]

In mice, *Snf5*-deficiency results in embryonic lethality by E6.5, while ~15% of $Snf5^{+/-}$ mice develop rhabdoid-like tumors at 8–10 months of age.[8] Conditional *Snf5* inactivation results in complete bone marrow aplasia leading to anemia, hemorrhage and death of most mice 1–3 weeks after induction.[9] Furthermore, SNF5 appears essential for hepatocyte differentiation based on the phenotype of hepatocyte-specific *Snf5* deletion in utero.[10] These data demonstrate that *Snf5* is

Key words: pediatric cancers, SWI/SNF complex, mouse models of cancer, SNF5/INI1
Additional Supporting Information may be found in the online version of this article.
This study characterizes the first MRT cell lines derived from genetically engineered mouse models as well as the effects of genetic background on *in vivo* MRT development. These cell lines will provide critical new reagents for dissecting the mechanisms that drive the epigenetic instability found in these unique tumors as well as serve as biological models for testing novel drugs for the treatment of this aggressive disease
Grant sponsor: PHS; **Grant numbers:** R01CA091048, R01CA113794, U01CA105423, RR00163; **Grant sponsor:** The Garrett B. Smith Foundation, Cure AT/RT Now Fund, Children's Tumor Foundation
DOI: 10.1002/ijc.27976
History: Received 14 May 2012; Accepted 7 Nov 2012; Online 29 Nov 2012
Correspondence to: Bernard E. Weissman, Lineberger Cancer Center, Room 32-048, University of North Carolina, Chapel Hill, NC 27599-7295, USA, Tel: +919-966-7533, Fax: +919-966-9673, E-mail: weissman@med.unc.edu

What's new?

Malignant rhabdoid tumors (MRTs) are rare, extremely aggressive cancers occurring in young children primarily through inactivation of the *SNF5 (INI1, SMARCB1)* tumor suppressor gene. This study characterizes the first MRT cell lines derived from genetically engineered mouse models as well as the effects of genetic background on in vivo MRT development. These cell lines will provide critical new reagents for dissecting the mechanisms that drive the epigenetic instability found in these unique tumors as well as serve as biological models for testing novel drugs for the treatment of this aggressive disease.

not only an MRT tumor suppressor, but also plays a critical role in both organ and cell differentiation.

Re-expression of SNF5 in SNF5-deficient human MRT cell lines reduces phosphorylation of the retinoblastoma protein (pRb) through activation of $p16^{INK4a}$ transcription and/or inhibition of cyclin D1 expression, leading to suppression of activating E2Fs.[8] The Rb/E2F pathway regulates cell cycle progression and plays an important role in a wide array of human cancers.[11,12] A recent *in vivo* study also suggests that Rb is epistatic to SNF5 in tumor suppression.[13]

Previous studies suggest that SNF5 loss might also contribute to the development of choroid plexus carcinoma (CPC),[14,15] a rare pediatric tumor of the active transport epithelium located in the brain ventricles. However, since MRTs often develop in similar locations and can be difficult to diagnose based on histology alone, there is some debate as to whether MRTs and CPCs are distinct tumors both impacted by SNF5 inactivation, tumor types that share a common origin, or unrelated tumors with histological similarities that cloud diagnosis (see Discussion). Therefore, we utilized a genetically engineered mouse model (GEMM), TgT_{121}, in which CPCs develop with high frequency to investigate whether loss of SNF5 contributes to CPC progression.

TgT_{121} mice express a truncated SV40 large T antigen (T_{121}) that inactivates pRb and related proteins p107 and p130 (but not p53) under the control of the lymphotropic papovavirus (LPV) promoter.[16] Transgene expression is robust in the choroid plexus epithelium (CPE), predisposing to CPC, and in B and T lymphoid cells without consequence.[16,17] Dominant interference of pRb, p107 and p130 by T_{121} is an effective strategy for complete inactivation of pRb family (pRb_f) function in the mouse due to compensation of pRb inactivation by p107 and/or p130.[18–20] TgT_{121} mice develop CPCs upon spontaneous CPE p53 inactivation and become terminal around 7 months of age.[21,22]

Here, to examine the combined effects of pRb_f and SNF5 inactivation and to determine the relationship (if any) between CPC and MRT, we analyzed development of these tumor types in TgT_{121};$Snf5^{+/-}$ mice. We report interesting tumor-specific differences in the co-operativity of these events. The results further provide insight into the MRT target cell type and the relationship between CPCs and MRTs.

Material and Methods

Generation of TgT_{121};$Snf5^{+/-}$ mice

The generation, screening and characterization of TgT_{121} transgenic and $Snf5^{+/-}$ mice were described previously.[16,21,23] TgT_{121} mice were maintained on a BDF1 (Jackson Labs, Bar Harbor, ME) background. We backcrossed the $Snf5^{+/-}$ mice to C57BL/6 mice for at least nine generations to produce congenic $Snf5^{+/-}$ mice. TgT_{121};$Snf5^{+/-}$ mice were derived by crossing TgT_{121} mice with $Snf5^{+/-}$ mice and using only F1 generation mice. Mice with resulting genotypes, TgT_{121}, $Snf5^{+/-}$, TgT_{121};$Snf5^{+/-}$ and TgT_{121};$Snf5^{+/+}$ were born with the expected Mendelian frequencies. All procedures approved by the Institutional Animal Care and Use Committees.

Genotyping

Mice were genotyped by PCR amplification of genomic DNA from either mouse tails or cell lines. Mouse genomic DNA was extracted by incubating tissues with buffer A (0.2 mM EDTA pH 8.0 and 25 mM NaOH) at 95°C for 1 hr. The lysate was neutralized by the same volume of buffer B (40 mM Tris-HCl) followed by vigorous vortexing. Debris was pelleted and the supernatant was used in PCR amplification. PCR was performed using the EasyStart 50 PCR Kit (Molecular Bio-Products Inc., San Diego, CA). The wild type *Snf5* allele were detected using primers against a sequence before exon 1 (Snf5-01 5′-CACCATGCCCCCACCTCCCCTACA-3′) and exon 1 (Snf5-02 5′-CAGGAAAATGGATGCAACTAAGAT-3′), while the *Snf5* null allele was amplified using primers against the neo insert (in exons 1-2; 5′-GGCCAGCTCATTCCTCCCACTCAT-3′) and Snf5-01. T121 positive animals were detected by using primers: 5′-GAATCTTTGCAGCTAATGGACC-3′ and 5′-GCATCCCAGAAGCTCCAAAG-3′. PCR conditions were: 94°C 1 min, 61°C or 59°C 2 min and 72°C 1 min for 35 cycles. Agarose gel electrophoresis was used to detect the PCR products.

Genomic DNA isolation and LOH analysis of Snf5

Tumor DNA was isolated from frozen tumor samples or from paraffin embedded tissue slices by using the DNeasy tissue kit (Qiagen, Valencia, CA). For primary tumors, samples were crushed into a fine power under liquid nitrogen prior to DNA isolation. Amplification of the *Snf5* wild type and null alleles by PCR was performed using the EasyStart 50 PCR Kit (Molecular Bio-Products, San Diego, CA) using the conditions described above.

Western blot analysis

Western blotting was carried out as previously described.[24] Briefly, protein concentration was quantified by the Bio-Rad protein assay (Bio-Rad Laboratories, Hercules, CA). Thirty-

five μg of protein were separated by electrophoresis on 4–20% SDS-polyacrylamide gels (Cambrex, East Rutherford, NJ) and electro-transferred onto immobilon-P membranes (Millipore, Billerica, MA) as per manufacturers' directions. Western analyses of proteins were carried out by using anti-$p16^{INK4a}$ (1:500, G175-1239, Pharmingen, San Diego, CA), anti-smooth muscle actin (1:200, Clone 1A4, Sigma, St. Louis, MO), anti-SV40 T antigen (1:1000, Pab416, Calbiochem, Darmstadt, Germany), anti-BAF180 (1:2,000, kind gift of Dr. Ramon Parsons, Columbia University), anti-Nestin (1:5,000, sc23929, SCBT, Santa Cruz, CA), anti-SOX2 (1:3,000, AB5603, Millipore, Billerica, MA), anti-$p18^{INK4C}$ (1:1,000, a kind gift from Dr. Xue Xiong, UNC-Chapel Hill), SNF5 (1:1,000, 612110, BD Biosciences, San Jose, CA), anti-ß-actin (1:4,000, A2066, Sigma, St. Louis, MO), and 1:2,000 horseradish peroxidase conjugated anti-rabbit or anti-mouse IgG (Amersham, Piscataway, NJ). Individual proteins were detected with ECL chemiluminescense reagent (Amersham, Piscataway, NJ) on Biomax ML film (Kodak, Rochester, NY).

Histopathology and Immunohistochemistry

Brain and facial tumors were fixed in 10% formalin for 16–20 hr, washed in running water for 3 min and saved in 70% ethanol. Tissues were routinely processed and embedded, and 5 μM sections were stained with hematoxylin and eosin (H&E) or immunohistochemistry (IHC) as described. For IHC, antigen retrieval was performed with 1.0 mM EDTA, pH 8.0 (Zymed, South San Francisco, CA) in a steam pressure cooker at 125°C for 30 sec followed by a cool down set point at 90°C for 10 sec (Decloaking Chamber, BioCare Medical, Walnut Creek, CA) as per manufacturer's instructions, followed by washing in distilled water. All further steps were performed at room temperature in a hydrated chamber. Slides were pretreated with Peroxidase Block (DAKO USA, Carpinteria, CA) for 5 min to quench endogenous peroxidase activity. For SNF5, monoclonal mouse anti-SNF5 antibody (BD Bioscience, clone 25/BAF47, Cat No. 612111) was applied at 1:100 in Dako diluent for 1 hr. Slides were washed in 50-mM Tris-HCl, pH 7.4, and detected with anti-mouse Envision+ kit (DAKO) as per manufacturer's instructions. After further washing, immunoperoxidase staining was developed using a DAB chromogen (DAKO) and counterstained with hematoxylin. H&E and IHC-stained sections were evaluated independently by experienced M.D. and D.V.M. pathologists (C.D.M.F. and A.B.R.) in blinded fashion.[23,25]

Immunocytochemistry

Cells grown on glass coverslips were fixed in ice-cold 4% paraformaldehyde in PBS for 15 min then washed three times with PBS. Cells were then incubated in blocking buffer (PBS with 5% normal goat serum and 0.1% Triton X-100) for 30 min at room temperature, then with the following primary antibodies for 1 hr: anti-GFAP (1:2,500; Dako), anti-neurofilament (NF-L; 1:1,500, Chemicon), anti-cleaved caspase 3 (1:1,000, Cell Signaling) or anti-S100β (1:1,000; Sigma), each diluted in blocking buffer. Following three washes in blocking buffer, cells were incubated with fluorescently labeled secondary antibodies (Alexa Fluor 488, 546; Molecular Probes, Eugene, OR, USA; diluted 1:2,500 in blocking buffer) for 30 min and counterstained with 4′,6-diamidino-2-phenylindole (DAPI) to label cell nuclei. Cells were then washed three times in PBS and mounted in fluoromount G (Southern Biotech, Birmingham, AL). Controls included sections incubated with no primary or secondary antibody and also with mismatched secondary and primary antibodies. For determination of apoptotic rates, three random fields of each cell line were counted.

Cytogenetic analyses

Cytogenetic analyses were carried out by KaryoLogic (Research Triangle Park, NC) following previously published protocols.[26]

In vitro growth curves

The *in vitro* growth rates were carried out as previously described.[27] Briefly, cells (5×10^5) were plated in normal growth medium in triplicate into 12-well cell dishes. At each indicated time, cells were harvested by trypsinization, rinsed with PBS and resuspended in 1 ml serum-free medium. Cell numbers were determined with a Coulter Counter apparatus.

In vivo growth assay

About 1×10^8 cells for each cell line were harvested by trypsinization, rinsed with PBS and resuspended in 1 ml serum-free medium. Six-week old *SoxN1 Nu/Nu* female mice were inoculated subcutaneously on the left and right abdomen with 100 μl (1×10^7 cells/site) of cell suspension. Mice were monitored daily for signs of distress and measured for tumor development 3× weekly. Mice were sacrificed when tumors reached a maximum dimension (height, width or length) of 2 cm.

Results

$Snf5^{+/-}$ and TgT_{121};$Snf5^{+/-}$ mice develop both facial and CNS-MRTs

Our previous study showed a significant decrease in the average latency for MRT development in TgT_{121};$Snf5^{+/-}$ mice compared to their $Snf5^{+/-}$ cohorts.[28] We also observed at least a ten-fold increase in the frequency of MRTs located around the dorsal roots or spinal nerves within the spinal cord, most frequently near the thoracolumbar junction in the TgT_{121};$Snf5^{+/-}$ mice.[28] We did not detect a significant change in the rate of appearance of facial MRTs and no evidence of intracranial MRT development.

A previous report by Klochlendler-Yeivin *et al.* indicated that genetic background may influence the frequency and the site of MRT development in $Snf5^{+/-}$ mice.[29] In our previous study, the $Snf5^{+/+}$ mice were maintained on a stable but undetermined mixed genetic background of C57BL/6 and 129/SvJ.[23,28,29] In order to minimize the effects of genetic

Table 1. Type, frequency and time to appearance of tumors in the $Snf5^{+/-}$ and TgT_{121};$Snf5^{+/-}$ mice

Genotype	Tumor/location		No. with tumors (total no.)	Median age (months)	Penetrance
TgT_{121};$Snf5^{+/-}$	CPC		8 ($n = 17$)	8.5	47%[1]
	MRT	Brain	3 ($n = 17$)	7.8	18%
		Soft tissue	3 ($n = 17$)		18%
$Snf5^{+/-}$	MRT	Brain	3 ($n = 14$)	14.4	21%
		Soft tissue	2 ($n = 14$)		14%

[1]This percentage does not include the six mice that were sacrificed due to the presence of MRTs. These mice also possessed CPCs at the time of autopsy.

background upon MRT development, we generated $Snf5^{+/-}$ mice on a congenic C57BL/6 background by backcrossing for greater than nine generations. We then crossed these mice to the TgT_{121} mice on a BDF1 background and followed TgT_{121};$Snf5^{+/-}$ and $Snf5^{+/-}$ F1 generation cohorts for up to 24 months. Similar to our previous study, TgT_{121};$Snf5^{+/-}$ mice developed tumors at a significantly younger age than the $Snf5^{+/-}$ mice (mean= 8.3 *vs.* 20.2 months, $p < 0.0001$) (Table 1).[22]

As shown in our previous report, we did not observe a significant difference in the penetrance of the MRTs between TgT_{121};$Snf5^{+/-}$ and $Snf5^{+/-}$ mice (Table 1).[28] Although the early onset of MRTs in many TgT_{121};$Snf5^{+/-}$ mice precluded determination of the CPC endpoint in these mice, we observed a comparable stage of CPC development at sacrifice to that previously reported for our TgT_{121} mice.[28] However, in constrast to our previous findings, we did not observe MRTs located around the dorsal roots or spinal nerves near the thoracolumbar junction.[28] Instead, the $Snf5^{+/-}$ and TgT_{121};$Snf5^{+/-}$ F1 C57/BL6.BDF1 mice developed an equal ratio of MRTs located in the soft tissues and in the brain (Table 1). Mesenchymal/rhabdoid-type tumors arose in the jaw, proximal foreleg and nasal cavity, whereas epithelial tumors with features of CPC were identified in the cerebellum and the cerebrum. Morphologic differentiation of the two tumor phenotypes was confirmed by both participating pathologists. Therefore, the cooperativity of pRb_f and SNF5 loss in MRT development again decreased tumor latency within tissues of the nervous system. However, the sites of these tumors apparently differed on the new genetic background.

MRTs but not CPCs show loss of SNF5 expression

Our previous studies had shown that loss of SNF5 expression accompanied the appearance of the MRTs in the TgT_{121};$Snf5^{+/-}$ mice.[28] In contrast, we did not observe loss of the wild-type SNF5 allele or protein expression in CPCs that arose in these mice.[28] To confirm that SNF5 loss only appeared in the MRTs in the TgT_{121};$Snf5^{+/-}$ mice, we carried out IHC to assess its expression in representative tumors. In Figure 1, right column, we show the histopathology of a representative CPC found in TgT_{121} mice.[16] Virtually all of the tumor cells show strong nuclear staining for SNF5 indicating retention of the wild-type *Snf5* allele. In contrast, the nuclei of the cells in representative malignant rhabdoid tumor show no evidence of SNF5 expression (Fig. 1, middle column). As we have previously observed, the tumors display a significant level of SNF5-positive inflammatory cells that serve as internal positive controls[30] (Fig. 1, middle column). We also saw positive nuclear staining for SNF5 in the unaffected areas of the brains of these mice (Fig. 1, left column).

Establishment of MRT cell lines from $Tg T_{121}$;$Snf5^{+/-}$ and $Snf5^{+/-}$ mice

Cell lines established from primary tumors have proven useful tools for dissecting the molecular events that lead to cellular transformation. In the case of MRT, a significant number of human MRT cell lines exist that have proven useful for understanding the role of SNF5 loss in tumor development.[8,31] However, despite the development of multiple GEMMs based upon constitutive or conditional loss of SNF5 expression, no mouse MRT cell lines have been reported. Therefore, we attempted to establish cell lines from primary MRTs of both genotypes and were able to successfully grow three cell lines.

The two cell lines, RTM639f and RTM658f, resembled the typical cellular morphology observed in many human MRT cell lines[32] (Fig. 2*a*). However, the RTM614f cell line showed a more fibroblast-like morphology, reminiscent of a 3T3 derived cell line. Therefore, we checked the genotype of each cell line to determine their consistency with the tumor of origin. As shown in Figure 2*b*, the RTM639f cell line, derived from a $Snf5^{+/-}$ MRT of the brain, and the RTM658f cell line, derived from a TgT_{121};$Snf5^{+/-}$ MRT near the scapula, had each lost the wild-type *Snf5* allele. However, the RTM614f cell line, derived from an explant of a TgT_{121};$Snf5^{+/-}$ facial MRT, had retained the wild-type *Snf5* allele (Fig. 2*b*). In agreement with the genotype results, both RTM658 and RTM639 do not express SNF5 protein while the RTM614 cell line does (Fig. 2*c*). Furthermore, both RTM614 and RTM658 express the T_{121} protein, in agreement with our previous report[28] (Fig. 2*c*). Therefore, we did not further characterize the RTM614 cell line because it appeared to arise from stromal contamination. The MRT cell lines have now grown for >20 passages in culture suggesting that they have attained immortality.

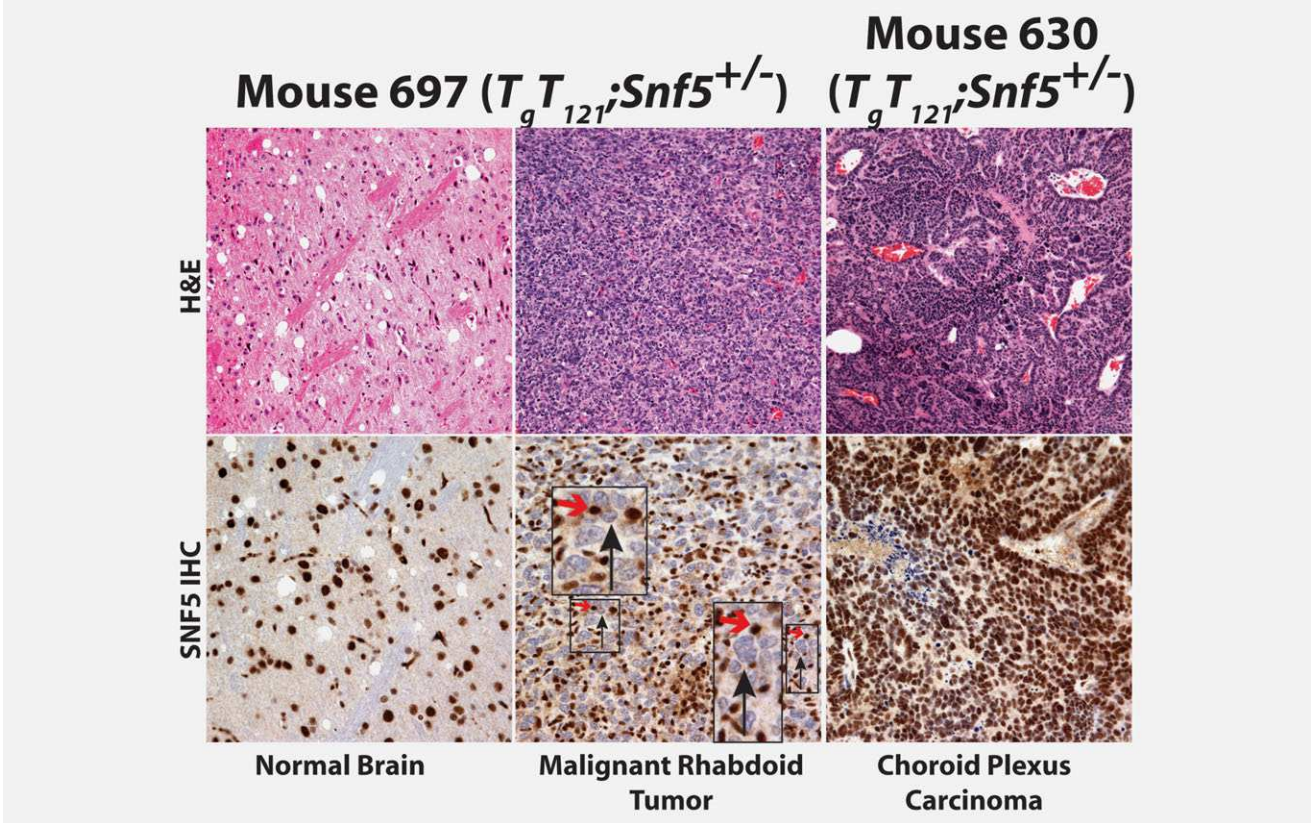

Figure 1. Histopathology and SNF5 immunohistochemistry of normal brain, MRT and CPC in TgT121;Snf5+/− mice. Paraffin-embedded sections of representative MRT, CPC and normal brain samples were stained for histology by H&E by standard methods (top row). Additional sections were also assessed for expression of SNF5 by immunohistochemistry as outlined in the Material and Methods in the bottom row. The red arrows denote SNF5-positive infilitrating immune cells while the black arrows show the larger nuclei of the MRT cells. The middle row demonstrates staining of sections in the absence of the primary anti-SNF5 monoclonal antibody. [Color figure can be viewed in the online issue, which is available at wileyonlinelibrary.com.]

Characterization of MRT cell lines

Differentiation marker expression. We examined both cell lines for expression of proteins associated with human MRTs. As shown in Figure 2*d*, the RTM658 and RTM639 cell lines expressed α-smooth muscle actin (αSMA), a protein reported as commonly expressed in human MRT cell lines.[33] Surprisingly, they also showed high levels of the cyclin-dependent kinase inhibitor (CDKI) protein $p16^{INK4A}$, a gene that remains silenced by polycomb in many human MRT cell lines.[24,34] As controls, we also confirmed expression of another CDKI protein, $p18^{INK4C}$, and a SWI/SNF complex member BAF180/PBRM1 (Fig. 2*d*).

A recent report implicated neural stem cells as the cell of origin for MRTs.[35] Furthermore, early histological characterizations of human MRTs demonstrated expression of neuronal differentiation markers.[36] Our previous analyses of protein expression in primary tumors from $Snf5^{+/-}$ and TgT_{121};$Snf5^{+/-}$ mice had also suggested a neuronal origin for these tumors.[28,30] We could not detect expression of two markers associated with neural differentiation, NESTIN and SOX2, in the RTM639f and RTM658f cell lines (Fig. 2*d*). However, both cell lines expressed glial fibrillary acidic protein (GFAP), a protein expressed by both mature glial cells and by neural progenitor cells (Fig. 2*e*). The RTM658f cell line also expressed S100ß, which is associated with differentiated Schwann cells in the peripheral nervous system and neurons in the central nervous system, and NF-L, a marker associated with differentiated neurons. In contrast, the RTM639f cell line weakly expressed NF-L in a subset of cells and lacked S100ß protein. These differences in neural marker differentiation may reflect the different anatomical site of origin of the two cell lines (see Discussion).

Cytogenetics. Human MRTs often display little evidence of genomic instability either at the level of cytogenetics or molecular markers.[37,38] Therefore, we examined the karyotypes of the mouse MRT cell lines by standard cytogenetic G-banding analysis to determine whether they had undergone significant genomic instability. As shown in Figure 3*a*, the RTM639f cell line retained a near diploid karyotype with a minimal number of chromosomal abnormalities (Supporting Information Fig. 1*a*). This relatively minor effect on gross genomic stability mirrors that observed in human MRT cell lines.[39,40] In contrast, the RTM658f cell line showed a hypotetraploid chromosome count although with minimal aberrant chromosomal rearrangements (Fig. 3*b*, Supporting

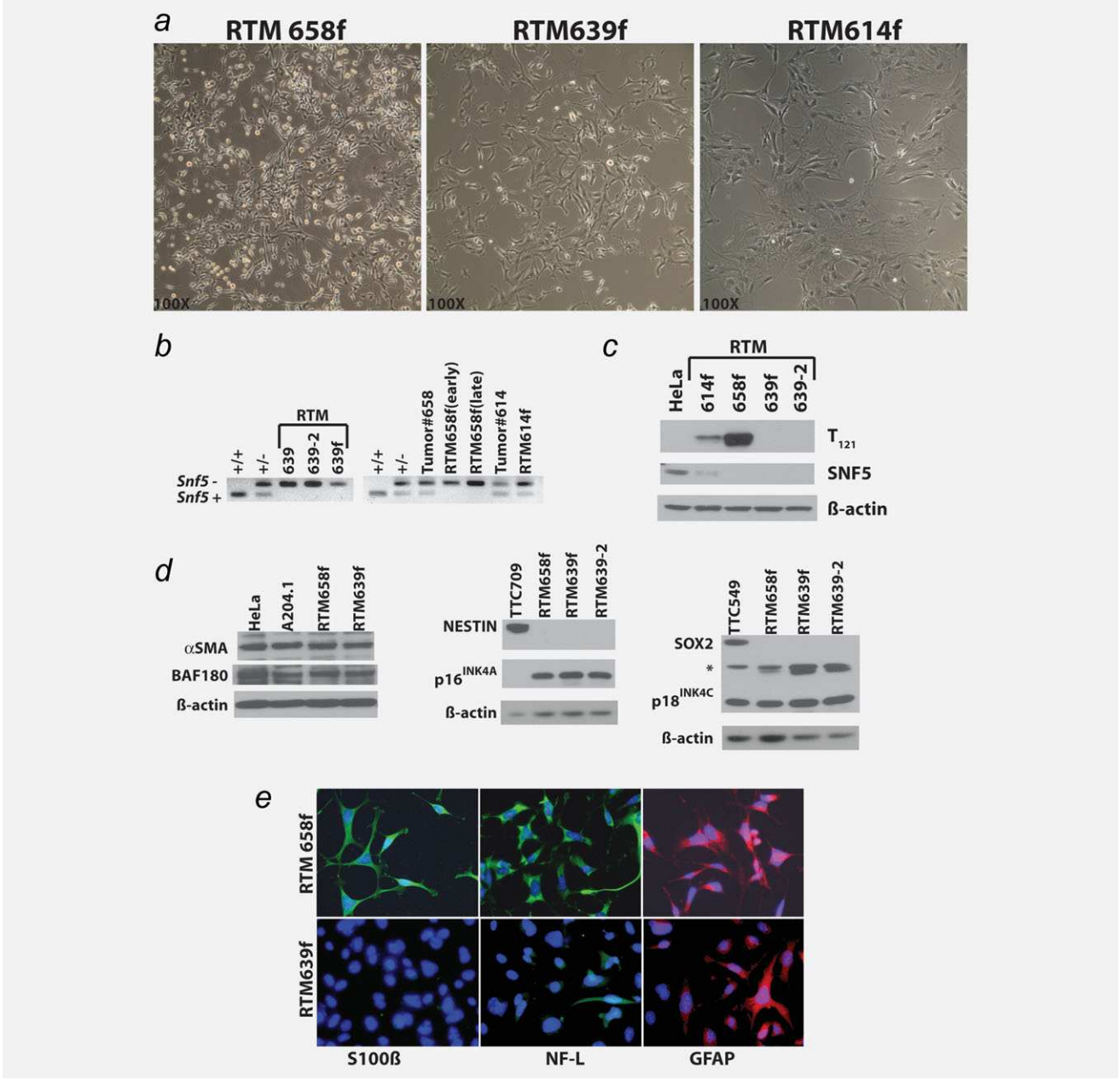

Figure 2. *In vitro* characterization of mouse MRT cell lines. (*a*) Photomicroscopy of the MRT-derived cell lines; (*b*) primary tumor and cell line genotyping: DNA was isolated from primary MRT samples and associated cell lines and assayed for the presence of wild-type and mutant SNF5 alleles by PCR analysis. The RTM639 and RTM639-2 cell lines were established independently in different flasks from the same MRT. RTM639f, RTM614f and RTM658f cell lines were subsequently isolated from the original cell line flask as a detached cell population to minimize fibroblast contamination. RTM658f (early): early passage, (late): late passage; (*c*) T121 expression: T121 protein expression in each cell line was assessed by Western blot analysis as described in the Material and Methods; (*d*) expression of differentiation and cell cycle markers: protein expression of cell cycle regulators $p16^{INK4A}$ and $p18^{INK4C}$, the SWI/SNF complex member and tumor suppressor BAF180/PBRM1 and the differentiation markers smooth muscle actin (SMA), SOX2 and NESTIN were determined by standard Western blotting protocols; (*e*) neural differentiation: neural differentiation was assessed by immunocytochemistry for NESTIN, GFAP and NF-L as described in the Material and Methods. Cells were visualized by fluorescence microscopy. [Color figure can be viewed in the online issue, which is available at wileyonlinelibrary.com.]

Information Fig. 1*b*). We analyzed the RTM-658f cell line at two different passage numbers, 21 and 52. While the relative chromosomal contribution to each karyotype was similar at both passages, we noted the appearance of dicentrics suggesting a significant level of genomic instability. We only examined the karyotype of the RTM-639f cell line at passage 23. However, we did not find any evidence of genomic instability in this cell line. The difference between the two cell lines may reflect the loss of Rb family function *via* expression of the T121 protein in the RTM658f cell line.

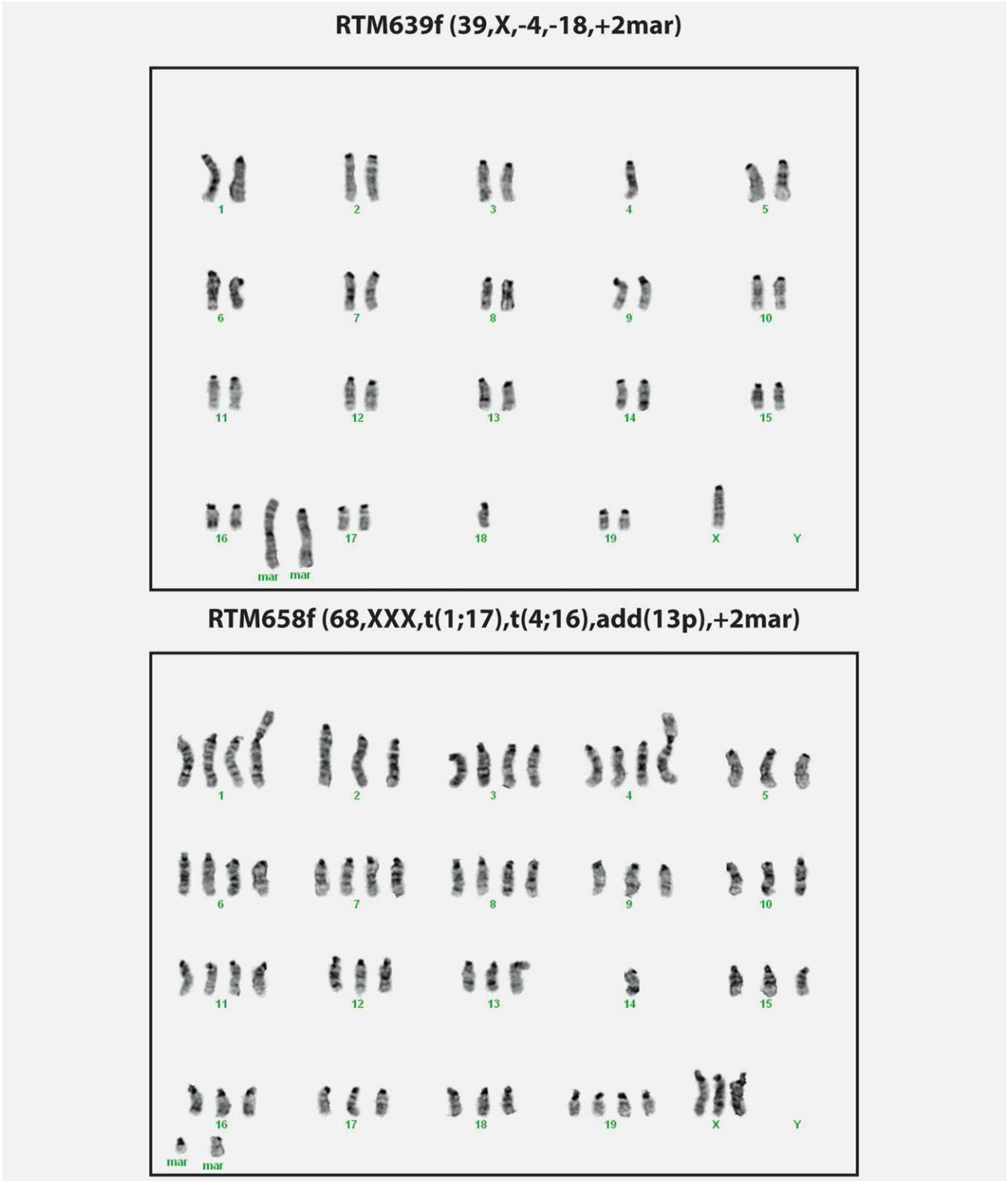

Figure 3. Representative karyotype of mouse MRT cell lines. Identification and characterization of the chromosome content of each cell line was performed using the standard G-banding method. Representative karyotypes of RTM-639f, passage no. 23 and RTM-658f, passage no. 52 are shown. [Color figure can be viewed in the online issue, which is available at wileyonlinelibrary.com.]

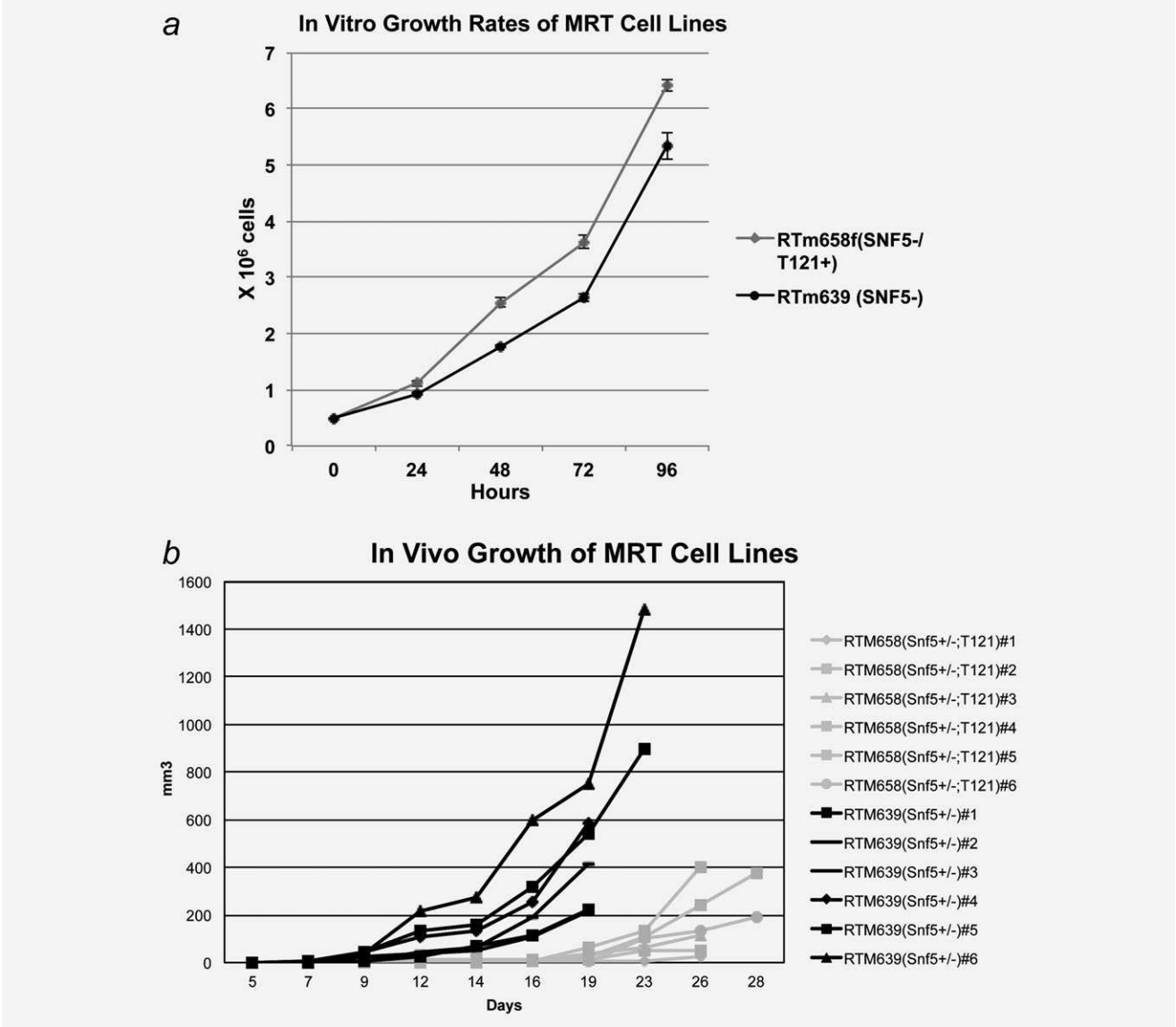

Figure 4. *In vitro* and *in vivo* growth rates of mouse MRT cell lines. (*a*) Each cell line was plated at 5×10^5 cells per well. On the designated days, cells were removed by treatment with trypsin-EDTA and counted by a Coulter Counter apparatus. A representative growth curve from duplicate biological experiments is presented. (*b*) Each cell line was inoculated S.C. into 6 *SoxN1 Nu/Nu* female mice and measured for tumor development 3× weekly. Each line represents the tumor growth of one subcutaneous inoculation per animal.

In vitro growth properties. Due to the apparent differences in the cellular morphology displayed by the two cell lines, we determine whether they show different growth properties in culture. As shown in Figure 4*a*, the cell lines showed rates of proliferation in culture. The RTM-658f possessed a doubling time of 27.1 hr (±0.24) while the RTM-639f cell line has a doubling time of 30.4 hr (±0.67). We also determined the rate of apoptosis in each cell line by assessing cleavage of caspase 3 by immunofluorescence as previously described[41] (Supporting Information Fig. 2). As with the growth rates, the apototic rates for the two cells lines did not differ significantly- RTM-658f: 0.2% (±0.1%) *vs*. RTM-639f: 0.4% (±0.2%).

In vivo tumorigenicity. We next assessed the ability of each cell line to form tumors in immunocompromised mice after subcutaneous inoculation. Figure 4*b* shows that both cell lines rapidly formed tumors in *nu/nu* mice necessitating sacrifice of the animals within 1 month after inoculation. Furthermore, the RTM639f cell line, derived from the $Snf5^{+/-}$ mouse, proved far more aggressive than theT121-expressing, TgT_{121};$Snf5^{+/-}$-derived RTM658f cell line.

The histopathologies of the original malignant rhabdoid tumors from which the MRT cell lines were derived are shown in the top panels of Figure 5 and the tumors formed by each cell line are shown in bottom panels. The histology resembled the architecture of the tumor from which each cell

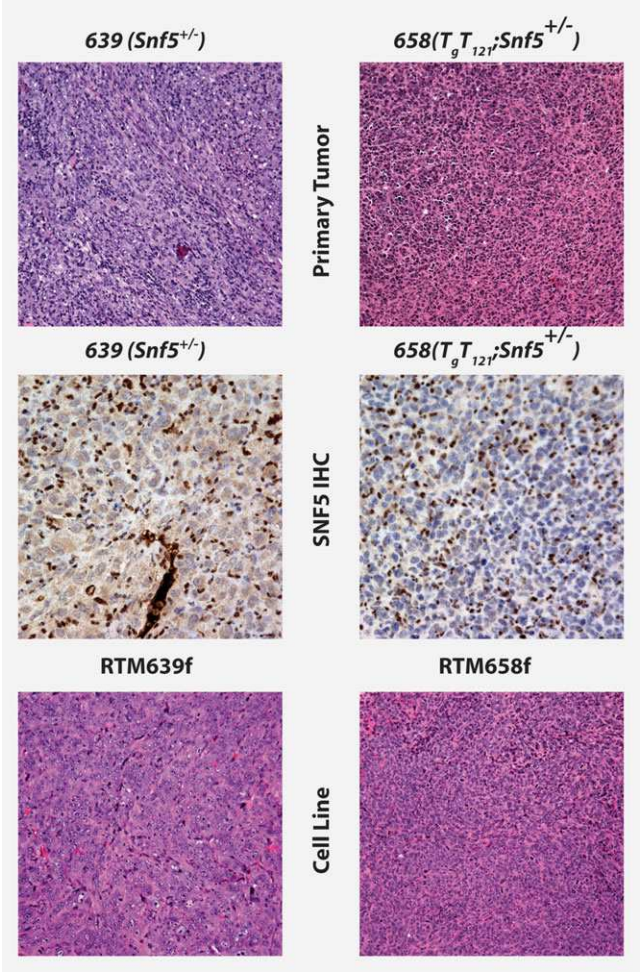

Figure 5. Histopathology and SNF5 immunochemistry of primary MRTs and MRT cell lines. Paraffin-embedded sections from the original tumors developed in the $Snf5^{+/-}$ mouse 639 and the $Snf5^{+/-}$;T_{121}, mouse 658 were stained for histology by H&E by standard methods (top row). Additional sections were also assessed for expression of SNF5 by immunohistochemistry as outlined in the Material and Methods in the middle row. In the bottom row, paraffin-embedded sections from tumors formed by the RTM639f and RTM658f cell lines in *Nu/Nu* mice were stained for histology by H&E as described above. [Color figure can be viewed in the online issue, which is available at wileyonlinelibrary.com.]

line was originally derived (Fig. 5—compare top and bottom panels). We confirmed genotyping and protein expression data from Figures 2*b* and 2*c* by IHC, demonstrating a loss of SNF5 protein expression in the original tumors (Fig. 5, middle panels). Therefore, these cell lines recapitulate the basic *in vivo* growth properties of the original MRT counterparts.

Discussion

While MRTs present as aggressive, embryonic neoplasms that may appear in a wide range of anatomical locations, almost all share an alteration of the *SNF5* gene resulting in protein loss.[31] Genetically engineered mouse models based upon inactivation of the *Snf5* gene have also shown a range of anatomical sites of MRT development including legs, face, spinal cord and brain.[23,29,42] However, the penetrance of tumor development as well as the range of anatomical sites with tumors differed among these reports.

One difference among the $Snf5^{+/-}$ GEMM characterized in the previous studies lies in the mixed genetic background of the mice. While all the models came from a cross between C57BL/6 and 129/SvJ mice, the actual contribution of each genome to the models is unknown. Thus, the differences observed among the three reports may arise from a difference in genetic background. Multiple reports have shown the influence of genetic background on tumor development in GEMMs.[43] Our current report supports this notion. While our previous study demonstrated MRTs on the face and the spinal cord at an average age of 4.5 months in TgT_{121};$Snf5^{+/-}$ mice, our current study showed MRTs on the face and in the brain at an average age of 7.8 months[28] (Table 1). The major difference between the two studies comes from the genetic backgrounds of the $Snf5^{+/-}$ mice-mixed C57BL/6x129SvJ *vs*. congenic C57BL/6. These results implicate genetic modifier loci that may influence both the rate of MRT development as well as the site of tumor initiation.

Primary human MRTs and human MRT cell lines display a remarkable chromosome and genomic stability.[37,38,40,44] In contrast, most mouse cell lines, including well-characterized "normal" cells such as NIH/3T3 and C3H10T1/2, possess aneuploid karyotypes.[45,46] However, like their human counterparts, the mouse MRT cell line RTM639 remained primarily diploid with only a minor amount of chromosome rearrangements. Interestingly, Lu *et al.* did not observe chromosomal instability in a Tg121 GEMM for choroid plexus development.[22] However, they did not examine cell lines established from these mice.

The cell of origin for MRTs remains unclear. Previous reports of $Snf5^{+/-}$ GEMMs have suggested that tumors have arisen from cells of neural crest origin in the mice.[28,42] Consistent with the *in vivo* tumor characterization, we observe expression of neural differentiation markers in the mouse MRT cell lines (Fig. 2). Of interest, the RTM639 cell line, derived from the brain, showed a differentiation expression pattern consistent with a neural progenitor.[47–49] However, the RTM658 cell line, derived from a facial tumor, showed a more differentiated pattern, expressing both neuronal and glial markers. Whether this difference reflects the site of origin of the tumors or the presence of the TgT_{121} transgene in the RTM658 cell line remains an open question.

The availability of GEMMs and cell lines that could lead to the identification of secondary genetic changes that influence the clinical course of MRT development in human patients offers the opportunity to address several important issues. Patients with MRT show a range of responses to treatment from little benefit to multiple years of remission. The differences in the rate of tumor development and the

penetrance observed in these GEMMs may provide insight into the genetic loci that influence how these tumors respond to therapy. We are currently developing *Snf5*$^{+/-}$ mice on a congenic 129SvJ background to directly compare the development of MRTs to the C57BL/6 background. Questions also remain about the relationship among MRTs (AT/RTs) that develop in different organ sites *i.e.*, do they represent the same tumor or different tumors with a common genetic defect? An expanding repitoire of GEMMs that develop MRTs in different sites may offer the means to experimentally address this issue by tracking the cell of origin in each model. Finally, the development of the mouse MRT cell lines will present a tractable system for rapidly testing new treatments in culture paired with a matched clinically relevant *in vivo* model.

Acknowledgements

We wish to thank Mr. Nisarg Desai for excellent help with the genotyping studies and the UNC-Lineberger Animal Studies Core for their help with the in vivo tumorigenicity studies. The work was supported by PHS awards R01CA091048 (B.E.W.), R01CA113794 and U01CA105423 (C.W.M.R.) and RR00163 (L.S.S.). Dr. Roberts also gratefully acknowledges support from The Garrett B. Smith Foundation and the Cure AT/RT Now fund. Dr. Sherman also gratefully acknowledges support from the Children's Tumor Foundation.

References

1. Weeks DA, Beckwith JB, Mierau GW. Rhabdoid tumor. An entity or a phenotype? *Arch Pathol Lab Med* 1989;113:113–14.
2. Savla J, Chen TT, Schneider NR, *et al.* Mutations of the hSNF5/INI1 gene in renal rhabdoid tumors with second primary brain tumors. *J Natl Cancer Inst* 2000;92:648–50.
3. Tekkok IH, Sav A. Primary malignant rhabdoid tumor of the central nervous system—a comprehensive review. *J Neurooncol* 2005;73: 241–52.
4. Versteege I, Medjkane S, Rouillard D, *et al.* A key role of the hSNF5/INI1 tumor suppressor in the control of the G1-S transition of the cell cycle. *Oncogene* 2002;21:6403–12.
5. Hoot AC, Russo P, Judkins AR, *et al.* Immunohistochemical analysis of hSNF5/INI1 distinguishes renal and extra-renal malignant rhabdoid tumors from other pediatric soft tissue tumors. *Am J Surg Pathol* 2004;28: 1485–91.
6. Stojanova A, Penn LZ. The role of INI1/hSNF5 in gene regulation and cancer. *Biochem Cell Biol* 2009;87:163–77.
7. Bruder CE, Dumanski JP, Kedra D. The mouse ortholog of the human SMARCB1 gene encodes two splice forms. *Biochem Biophys Res Commun* 1999;257:886–90.
8. Wilson BG, Roberts CW. SWI/SNF nucleosome remodellers and cancer. Nature reviews. *Cancer* 2011;11:481–92.
9. Roberts CW, Leroux MM, Fleming MD, *et al.* Highly penetrant, rapid tumorigenesis through conditional inversion of the tumor suppressor gene Snf5. *Cancer Cell* 2002;2: 415–25.
10. Gresh L, Bourachot B, Reimann A, *et al.* The SWI/SNF chromatin-remodeling complex subunit SNF5 is essential for hepatocyte differentiation. *EMBO J* 2005;24:3313–24.
11. Gordon GM, Du W. Conserved RB functions in development and tumor suppression. *Protein Cell* 2011;2:864–78.
12. Chen HZ, Tsai SY, Leone G. Emerging roles of E2Fs in cancer: an exit from cell cycle control. Nature reviews. *Cancer* 2009;9:785–97.
13. Guidi CJ, Mudhasani R, Hoover K, *et al.* Functional interaction of the retinoblastoma and ini1/snf5 tumor suppressors in cell growth and pituitary tumorigenesis. *Cancer Res* 2006;66: 8076–82.
14. Zakrzewska M, Wojcik I, Zakrzewski K, *et al.* Mutational analysis of hSNF5/INI1 and TP53 genes in choroid plexus carcinomas. *Cancer Genet Cytogenet* 2005;156:179–82.
15. Sevenet N, Lellouch-Tubiana A, Schofield D, *et al.* Spectrum of hSNF5/INI1 somatic mutations in human cancer and genotype-phenotype correlations. *Hum Mol Genet* 1999;8:2359–68.
16. Saenz Robles MT, Symonds H, Chen J, *et al.* Induction versus progression of brain tumor development: differential functions for the pRB- and p53-targeting domains of simian virus 40 T antigen. *Mol Cell Biol* 1994;14:2686–98.
17. Pipas JM, Peden KW, Nathans D. Mutational analysis of simian virus 40 T antigen: isolation and characterization of mutants with deletions in the T-antigen gene. *Mol Cell Biol* 1983;3:203–13.
18. Lee MH, Williams BO, Mulligan G, *et al.* Targeted disruption of p107: functional overlap between p107 and Rb. *Genes Dev* 1996;10: 1621–32.
19. Robanus-Maandag E, Dekker M, van der Valk M, *et al.* p107 is a suppressor of retinoblastoma development in pRb-deficient mice. *Genes Dev* 1998;12:1599–609.
20. Sage J, Mulligan GJ, Attardi LD, *et al.* Targeted disruption of the three Rb-related genes leads to loss of G(1) control and immortalization. *Genes Dev* 2000;14:3037–50.
21. Symonds H, Krall L, Remington L, *et al.* p53-dependent apoptosis suppresses tumor growth and progression in vivo. *Cell* 1994;78:703–11.
22. Lu X, Magrane G, Yin C, *et al.* Selective inactivation of p53 facilitates mouse epithelial tumor progression without chromosomal instability. *Mol Cell Biol* 2001;21:6017–30.
23. Roberts CW, Galusha SA, McMenamin ME, *et al.* Haploinsufficiency of snf5 (integrase interactor 1) predisposes to malignant rhabdoid tumors in mice. *Proc Natl Acad Sci USA* 2000;97:13796–800.
24. Kuwahara Y, Charboneau A, Knudsen ES, *et al.* Reexpression of hSNF5 in malignant rhabdoid tumor cell lines causes cell cycle arrest through a p21(CIP1/WAF1)-dependent mechanism. *Cancer Res* 2010;70:1854–65.
25. Dai C, Whitesell L, Rogers AB, *et al.* Heat shock factor 1 is a powerful multifaceted modifier of carcinogenesis. *Cell* 2007;130:1005–18.
26. Koch J. Principles and applications of PRINS in cytogenetics. *Curr Protoc Hum Genet* 2004, Chapter 4: Unit 4 12.
27. Kuwahara Y, Hosoi H, Osone S, *et al.* Antitumor activity of gefitinib in malignant rhabdoid tumor cells in vitro and in vivo. *Clin Cancer Res* 2004; 10:5940–8.
28. Chai J, Lu X, Godfrey V, *et al.* Tumor-specific co-operation of retinoblastoma protein family and snf5 inactivation. *Cancer Res* 2007;67:3002–9.
29. Klochendler-Yeivin A, Fiette L, Barra J, *et al.* The murine SNF5/INI1 chromatin remodeling factor is essential for embryonic development and tumor suppression. *EMBO Rep* 2000;1:500–6.
30. DelBove J, Kuwahara Y, Mora-Blanco EL, *et al.* Inactivation of SNF5 cooperates with p53 loss to accelerate tumor formation in Snf5(+/−); p53(+/−) mice. *Mol Carcinog* 2009;48: 1139–48.
31. Roberts CW, Biegel JA. The role of SMARCB1/INI1 in development of rhabdoid tumor. *Cancer Biol Ther* 2009;8:412–16.
32. Betz BL, Strobeck MW, Reisman DN, *et al.* Re-expression of hSNF5/INI1/BAF47 in pediatric tumor cells leads to G1 arrest associated with induction of p16ink4a and activation of RB. *Oncogene* 2002;21:5193–203.
33. Kato H, Ohta S, Koshida S, *et al.* Expression of pericyte, mesangium and muscle markers in malignant rhabdoid tumor cell lines: differentiation-induction using 5-azacytidine. *Cancer Sci* 2003;94:1059–65.
34. Kia SK, Gorski MM, Giannakopoulos S, *et al.* SWI/SNF mediates polycomb eviction and epigenetic reprogramming of the INK4b-ARF-INK4a locus. *Mol Cell Biol* 2008;28:3457–64.
35. Gadd S, Sredni ST, Huang CC, *et al.* Rhabdoid tumor: gene expression clues to pathogenesis and potential therapeutic targets. *Lab Invest* 2010;90: 724–38.
36. Parham DM. Pediatric neoplasia: morphology and biologyed. Philadelphia: Lippincott-Raven, 1996.
37. McKenna ES, Sansam CG, Cho YJ, *et al.* Loss of the epigenetic tumor suppressor SNF5 leads to cancer without genomic instability. *Mol Cell Biol* 2008;28:6223–33.
38. Rousseau-Merck MF, Fiette L, Klochendler-Yeivin A, *et al.* Chromosome mechanisms and INI1 inactivation in human and mouse rhabdoid tumors. *Cancer Genet Cytogenet* 2005; 157:127–33.
39. Ota S, Crabbe DC, Tran TN, *et al.* Malignant rhabdoid tumor. A study with two established cell lines. *Cancer* 1993;71:2862–72.
40. Weissman BE, Saxon PJ, Pasquale SR, *et al.* Introduction of a normal human chromosome 11 into a Wilms' tumor cell line controls its tumorigenic expression. *Science* 1987;236: 175–80.

41. Matsumoto S, Banine F, Struve J, *et al.* Brg1 is required for murine neural stem cell maintenance and gliogenesis. *Dev Biol* 2006;289:372–83.
42. Guidi CJ, Sands AT, Zambrowicz BP, *et al.* Disruption of ini1 leads to peri-implantation lethality and tumorigenesis in mice. *Mol Cell Biol* 2001;21:3598–603.
43. Doetschman T. Influence of genetic background on genetically engineered mouse phenotypes. *Methods Mol Biol* 2009;530:423–33.
44. Karnes PS, Tran TN, Cui MY, *et al.* Establishment of a rhabdoid tumor cell line with a specific chromosomal abnormality, 46,XY,t(11;22)(p15.5;q11.23). *Cancer Genet Cytogenet* 1991;56:31–8.
45. Privitera E, Mosna G, Sala E, *et al.* Double minute chromosomes and a homogeneously staining chromosome region in C3H10T1/2 murine cells transformed "in vitro" by proton radiation. *Cancer Genet Cytogenet* 1990;49:75–86.
46. Kasid UN, Weichselbaum RR, Brennan T, *et al.* Sensitivities of NIH/3T3-derived clonal cell lines to ionizing radiation: significance for gene transfer studies. *Cancer Res* 1989;49:3396–400.
47. Laywell ED, Rakic P, Kukekov VG, *et al.* Identification of a multipotent astrocytic stem cell in the immature and adult mouse brain. *Proc Natl Acad Sci USA* 2000;97:13883–8.
48. Imura T, Kornblum HI, Sofroniew MV. The predominant neural stem cell isolated from postnatal and adult forebrain but not early embryonic forebrain expresses GFAP. *J Neurosci* 2003;23:2824–32.
49. Morshead CM, Garcia AD, Sofroniew MV, *et al.* The ablation of glial fibrillary acidic protein-positive cells from the adult central nervous system results in the loss of forebrain neural stem cells but not retinal stem cells. *Eur J Neurosci* 2003;18:76–84.